

Structure of densified amorphous germanium dioxide

This article has been downloaded from IOPscience. Please scroll down to see the full text article.

2004 J. Phys.: Condens. Matter 16 L131

(<http://iopscience.iop.org/0953-8984/16/10/L03>)

View [the table of contents for this issue](#), or go to the [journal homepage](#) for more

Download details:

IP Address: 129.252.86.83

The article was downloaded on 27/05/2010 at 12:48

Please note that [terms and conditions apply](#).

LETTER TO THE EDITOR

Structure of densified amorphous germanium dioxide**Matthieu Micoulaut**Laboratoire de Physique Théorique des Liquides, Université Pierre et Marie Curie, Boite 121,
4, Place Jussieu, 75252 Paris Cedex 05, France

E-mail: mmi@lptl.jussieu.fr

Received 17 December 2003

Published 27 February 2004

Online at stacks.iop.org/JPhysCM/16/L131 (DOI: 10.1088/0953-8984/16/10/L03)**Abstract**

Classical molecular dynamics simulations are used to study the structure of densified germanium dioxide (GeO_2). It is found that the coordination number of germanium changes with increasing density (pressure) while pressure released systems exhibit only a marked angular change in local structure as compared to the virgin system. The structural modification with pressure appears to be stepwise and gradually affects long-range (through the reduction of the long-range correlations as seen from the shift of the first sharp diffraction peak), intermediate-range (by angular reduction) and finally short-range structure (by tetrahedron distortion).

1. Introduction

Structural transitions in minerals are known to take place under various geological conditions [1, 2]. In the Earth's interior, silicate and alumino-silicate melts change their local structure causing strong density and viscosity modifications in magmas [3] and silicon exhibits at high pressure a change of its coordination number [4]. These results have been mostly obtained in high pressure–temperature experiments [5] but also in computer simulations [6] reproducing extreme conditions. Both have inferred the nature of these structural transitions, the structure and the phase portrait of the liquid state. However, while a majority of studies have been devoted to the silica and silicate chemistry, little has been done to elucidate the corresponding behaviour in germanium dioxide (GeO_2) even though this material is a structural analogue of silica in many respects: both materials exhibit at ordinary conditions a tetrahedral local structure, they can also exist in α as well as β quartz phases [7] and the change of germanium coordination from four to six also occurs at high pressure [8]. The structure of *in situ* densified or permanently densified GeO_2 remains, however, controversial. While the global increase with pressure of the germanium–oxygen distance in GeO_2 has been related from x-ray diffraction [8] with the conversion of tetrahedral Ge(4) into octahedral Ge(6), it seems that this structural change is reversible, as no Ge(6) is found in decompressed samples [9], a situation which does not occur [8] in decompressed rutile-like c- GeO_2 . The interest in

germanium coordination change has also been motivated by observation of the so-called ‘germanate anomaly’ which corresponds to a maximum in density and refractive index when 15–16 mol% Na₂O is added to the basic GeO₂ network former [10]. These binary systems have been investigated by various spectroscopic tools [11, 12] and it is suggested that the increasing presence of GeO₆ octahedra (Ge(6)) within the network is responsible for the anomaly. On the other hand, micro-Raman [13] spectroscopy applied to the same systems suggests that the anomaly is due to a massive conversion of 4-membered rings into more close-packed ones such as 3-membered rings, with no, or at least very few, Ge(6) present.

A preliminary task, if one wishes to describe density-induced structural changes in germanates, is first to understand how the basic network former GeO₂ changes with densification. While crystalline phases of GeO₂ have been studied in numerical calculations [14, 15], we are not aware of any published result on simulated liquid and amorphous GeO₂. It is therefore of striking interest to see what molecular dynamics (MD) can tell about a certain number of experimental open questions which remain at this stage. How does densification affect the local structure in the amorphous material? Which thermodynamical quantity (temperature, pressure) mostly controls the existence of a six-fold-coordinated germanium? Does octahedral germanium exist in pressure released (permanently densified) GeO₂? This letter attempts to address some of these basic issues by providing the first MD study of amorphous germania. The results show several main features. They demonstrate the reversible nature of pressure-induced changes in terms of bond distances, while the local coordination number of the germanium increases smoothly from 4 to 5.7 with applied pressure up to 30 GPa, a result that would be accessible from *in situ* experiments, as already realized for silica [16]. Furthermore, several regimes of densification can be clearly identified: a first regime ($P \leq 1.8$ GPa) during which no global change in the local structure is found to occur whereas the increase in the position of the first sharp diffraction peak (FSDP) suggests a global reduction of the longer-range correlations. In the window $1.8 \text{ GPa} \leq P \leq 2.8 \text{ GPa}$, a sharp decrease of the intertetrahedral bond angle permits the structure to be densified with no distortion of the basic GeO_{4/2} tetrahedron. This leads to the buckling of the network connected tetrahedra. Finally, for larger pressures, distortion of the tetrahedra sets in. As a consequence, additional constraints appear for $P > 3$ GPa which produce a global stiffening of the network [17, 18].

2. Simulation details

The system consists of 256 germanium and 512 oxygen atoms interacting via a Born–Huggins–Mayer type potential which has been fitted, in the case of GeO₂ by Oeffner and Elliot, to recover the crystalline phases of GeO₂ and its vibrational spectra [14]. Although monatomic systems such as crystalline germanium or diamond are unstable against a close-packed structure when described by any reasonable smooth two-body potential, many BX₂ (B = Si, Ge and X = O, Se, S) amorphous systems can easily be simulated at low and high pressure with this kind of interaction [19]. This arises mostly from the fact that there can be a charge transfer, due to the high polarizability, from the germanium atom to the oxygen atom resulting in the formation of Ge⁴⁺ and O²⁻ ions in the condensed phase. The simplest way to model these interactions is therefore to incorporate, besides the long-range Coulombic term, a steric repulsion (with a Ge size that is considerably smaller compared to oxygen) and a term containing the electronic polarizability of the ions considered. As pressurized silica [20] has been modelled with some success with this kind of two-body potential, we are confident that this can happen in GeO₂ as well.

The atoms have been first confined in a cubic box of length $L = 23.044 \text{ \AA}$ in order to recover the experimental value of the density ($\rho_g = 3.66 \text{ g cm}^{-3}$). After having thermalized

the system at 3000 K for 20 000 time steps (20 ps) the system has been cooled to 300 K with a linear cooling schedule at a quench rate of $2.5 \times 10^{12} \text{ K s}^{-1}$. Integration has been done using a leap-frog Verlet algorithm. Various configurations (positions and velocities) have been saved at different temperatures which have been used as starting configurations for production runs of 10^5 steps.

Densification has been realized reproducing experimental conditions, i.e. starting from an initial configuration at $T = 300 \text{ K}$ and ρ_g and increasing the density during 10^4 time steps. At the density ρ_g , the glass transition temperature was about 1010 K and, as expected, the T_g shifts to the higher temperatures with increasing density (1025 K at $\rho = 1.1\rho_g$). The sample data of Price and co-workers [12] have been almost recovered, i.e. after MD pressure release from 15.16 GPa determined from the virial¹. The final density of the decompressed system at zero pressure was $\rho = 4.5 \text{ g cm}^{-3} = 1.25\rho_g$. The corresponding configuration (called in the following the ‘*permanently densified system*’) was taken for comparison with the experimental study [21] of permanently densified GeO₂.

3. Results and discussion

The results for the partial structure factors $S_{ij}(Q)$ are displayed in figure 1 at $\rho_g = 3.66 \text{ g cm}^{-3}$ which show a fair agreement with the experimental results obtained from a combination of x-ray and neutron data [12]. One has to note, however, that these measurements have been refined but without any complete resolution of all the partials [21]. The principal features in the structure factors of GeO₂ are the peaks occurring at $Q_P = 1.5\text{--}2 \text{ \AA}^{-1}$ (the first sharp diffraction peak, FSDP, corresponding to a correlation length $L_1 = 2\pi/Q_P \simeq 4.1 \text{ \AA}$). Peaks at 2.6 and 4 \AA^{-1} appearing in the partial structure factors of the Ge–O and O–O can be associated with chemical short-range order (CRSO) and topological short-range order as derived from scaling considerations [22]. For the former, the similar height of $g_{\text{Ge–Ge}}$ and $g_{\text{O–O}}$ but with opposite signs suggests the CRSO nature of the network. The evolution of the total scattering function and the position of the FSDP with respect to pressure is discussed below.

The calculation of the pair correlation functions (figure 2) permits us to extract the simulated bond lengths which also agree with the experimental findings: $d_{\text{Ge–Ge}} = 3.32 \text{ \AA}$, $d_{\text{Ge–O}} = 1.72 \text{ \AA}$ and $d_{\text{O–O}} = 2.81 \text{ \AA}$ (to be respectively compared to the experimental values [11] of 3.16 ± 0.03 , 1.73 ± 0.03 and $2.83 \pm 0.05 \text{ \AA}$). Weak changes in Ge–Ge and Ge–O *bond distances* are found when comparing the virgin and the permanently densified system which yields $r_{\text{Ge–Ge}} = 3.34 \text{ \AA}$, $r_{\text{Ge–O}} = 1.71 \text{ \AA}$ and $r_{\text{O–O}} = 2.66 \text{ \AA}$, a result which is consistent with the experimental findings on $d_{\text{Ge–O}}$ of Itié *et al* [8]. The latter showed a global increase of the Ge–O bond distances from 1.73 \AA to the value 1.86 \AA at 29.1 GPa, typical of octahedral germania. The present simulation shows, however, only an increase up to 1.79 \AA for the same applied pressure of $\simeq 30 \text{ GPa}$ but the same constant value $d_{\text{Ge–O}} = 1.72 \text{ \AA}$ from 0 up to 8.91 GPa, in agreement with [8]. Here one is able to go beyond the simple description in terms of Ge–O bondings and we highlight several noticeable difference between virgin and permanently densified germania: the change in the Ge–Ge correlator is found to be moderate as seen from the shift of the first peak. On the other hand, $g_{\text{O–O}}$ not only shows a shift in bond distance ($\Delta d_{\text{O–O}} = 0.15 \text{ \AA}$) but also a loss in the peak heights that leads to a slight shift in the corresponding running coordination number $n_{\text{O–O}}$. The number of oxygen neighbours around a germanium atom is modified from 4.1 to 4.53, which corresponds to a respective mean fraction x_6 of six-fold-coordinated germanium atoms of 0.05 and 0.265.

Further differences are shown in the inset of figure 3 which displays a change in the mean bond angle Ge–O–Ge and O–Ge–O upon decompression. On a larger length scale, the most

¹ The pressure at 15.16 GPa has been obtained from a densified system at $\rho = 5.9 \text{ g cm}^{-3}$.

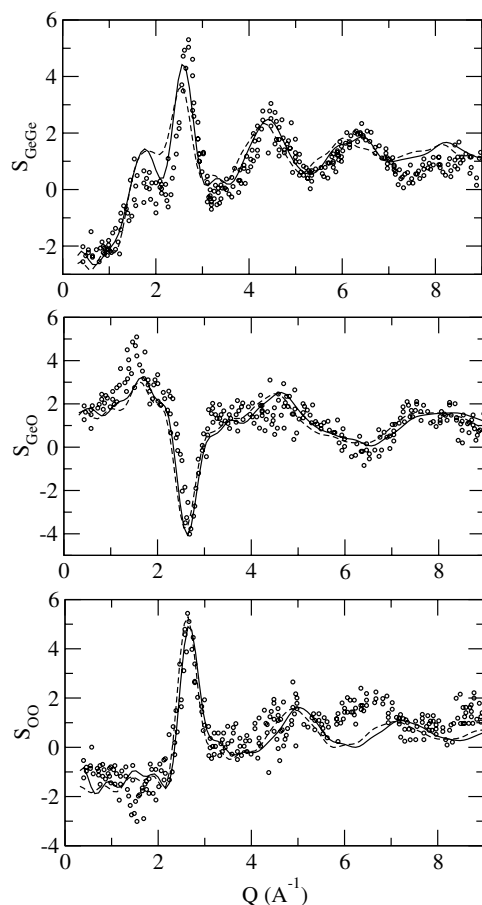


Figure 1. Partial structure factors $S_{ij}(Q)$ of vitreous germania at 300 K from MD simulations (full curve) at $\rho = \rho_g$ compared to experimental results (circles) from [11]. The broken curves represent the partial structure factors of the permanently densified system at $\rho = 1.25\rho_g$ (see the text for details).

noticeable difference is the disappearance of the first peak in the Ge–Ge partial structure factor, which grows from $Q_P = 1.77 \text{ \AA}^{-1}$ ($L_1 = 3.54 \text{ \AA}$) to a shouldered peak at $Q_P = 2.49 \text{ \AA}^{-1}$ ($L_1 = 2.52 \text{ \AA}$), leading to a global decrease of the longer-range correlation. The general discrepancy obtained between the virgin and permanently densified system is close to the one observed by Price and co-workers (specifically, see the different structure factors [21]).

More dramatic is the change in structure in the pressurized system at 16.6 GPa (dots in the insets of figure 2) which show substantial differences in the bond distances ($d_{\text{Ge-Ge}} = 3.25 \text{ \AA}$, $d_{\text{Ge-O}} = 1.75 \text{ \AA}$ and $d_{\text{O-O}} = 2.56 \text{ \AA}$) and an increase of the number of oxygen neighbours in the vicinity of a Ge atom (about 5.2, i.e. $x_6 = 0.60$, in the inset representing $n_{\text{Ge-O}}$, see also figure 4). The stressed upper limit of $n_{\text{Ge-O}} \simeq 6$ deduced from the corresponding bond distance at high pressure [8] is found to have a slow convergence in simulation, for example, for a computed $P = 29.3 \text{ GPa}$, $n_{\text{Ge-O}} = 5.70$ ($x_6 = 0.85$). Evidence of supplementary atoms in the first shell surrounding a central $\text{GeO}_{4/2}$ unit is also provided by the increase of $n_{\text{Ge-Ge}}$.

Using the present simulation, it is now possible to analyse in more depth the low pressure behaviour. The distortion of the tetrahedron parameter defined by $\delta_X = d_{\text{X-O}}/d_{\text{O-O}}$

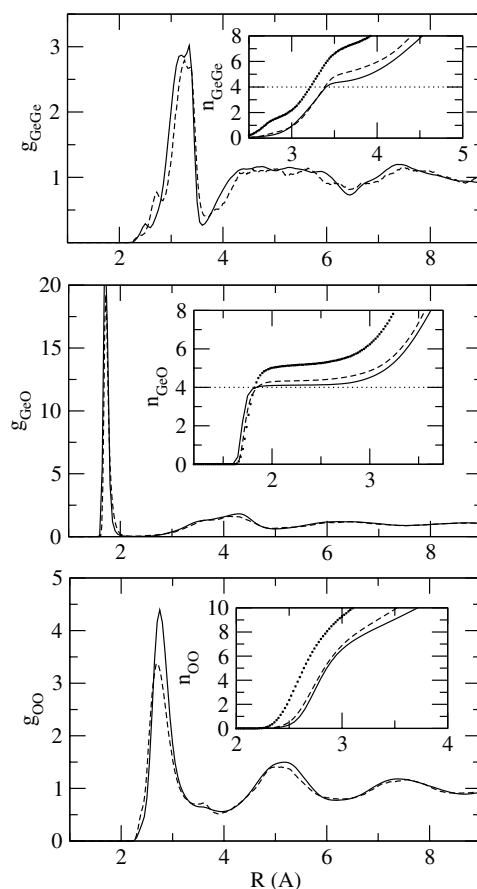


Figure 2. Calculated partial pair correlation functions in vitreous germania at 300 K at an ordinary density $\rho_g = 3.66 \text{ g cm}^{-3}$ (full curve) and in a permanently densified system ($\rho = 4.5 \text{ g cm}^{-3}$, broken curve). The inset represent the corresponding running coordination number $n_{ij}(R)$ together with results from a system under 16.6 GPa pressure (dots).

($X = \text{Si, Ge}$) which provides a direct measure of the effect of the pressure on the local structure of the network, is focused upon. For an ideal tetrahedron, $\delta = \sqrt{3/8}$. The latter quantity is of central interest when studying the flexibility of the glass under pressure [18] and the rigid unit modes in the context of pressure-induced rigidity [23, 24]. In figure 3 are represented the variation of the tetrahedron parameter δ_X with pressure for both silica [25]² and germania. At low pressure, δ_{Ge} remains almost constant, suggesting that the tetrahedral environment is preserved, slightly higher, however, than the value of a perfect tetrahedron. For $P \geq 2.8 \text{ GPa}$, there is increasing distortion of the tetrahedron in germania. The way of distortion appears, however, to be radically different compared to the silica system. In the former it is found as a stepwise increase (most noticeable from the jump of δ_{Ge} at around 3 GPa), in contrast with the more or less smooth increase of δ_{Si} . In the inset of figure 3 are shown the variation of the mean bond angles O–Ge–O and Ge–O–Ge with respect to pressure. As pressure is increased, the intratetrahedral bond angle decreases since the Ge–O bond distances increases. The constant

² The MD simulated silica glass has been studied under the same standard conditions described above and the potential reported by Tsuneyucki *et al* [25] starting from the ordinary density $\rho_g = 2.2 \text{ g cm}^{-3}$ and increasing density.

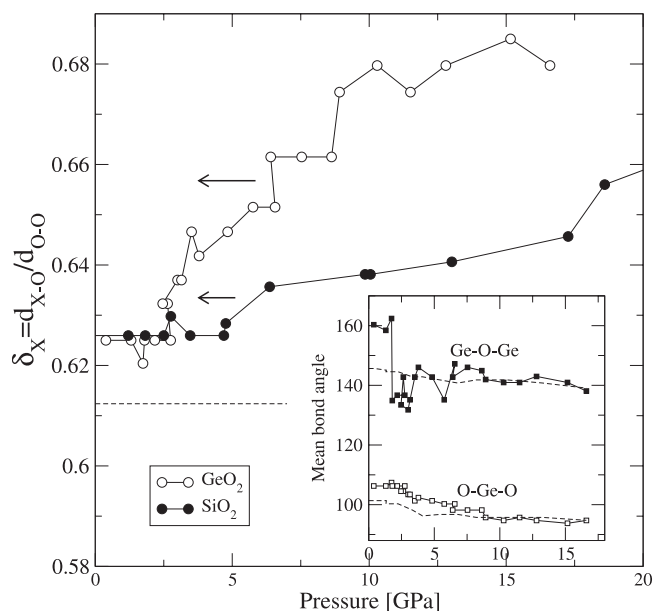


Figure 3. The distortion parameter of a regular $\text{GeO}_{4/2}$ as a function of applied pressure (open circles). For comparison, the same parameter for SiO_2 (full circles) is shown. The broken horizontal line represents the value $\sqrt{3/8}$. The inset shows the mean bond angles Ge-O-Ge and O-Ge-O with respect to compression (symbols) and decompression (broken curves).

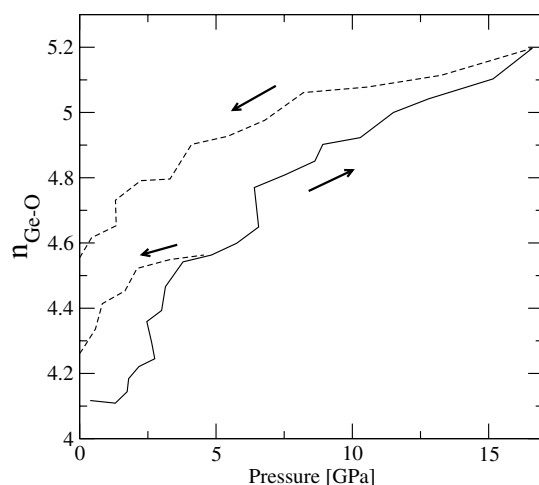


Figure 4. Ge–O coordination number under compression (full curve) and decompression (broken curves) from 4.8 and 16.6 GPa.

value of the O–Ge–O bond angle at low pressure correlates, of course, with the absence of distortion of the basic tetrahedron. The main feature provided by the angular analysis comes from the variation of the intertetrahedral mean bond angle Ge-O-Ge with pressure, which exhibits a sharp drop at around 1.8 GPa, from 158° to 135° , followed by a stabilization at around 140° . Densification first applies at the angles connecting the tetrahedra and leaves the O–Ge–O bond angle intact (or δ_{Ge} constant). If pressure keeps increasing, the distortion of

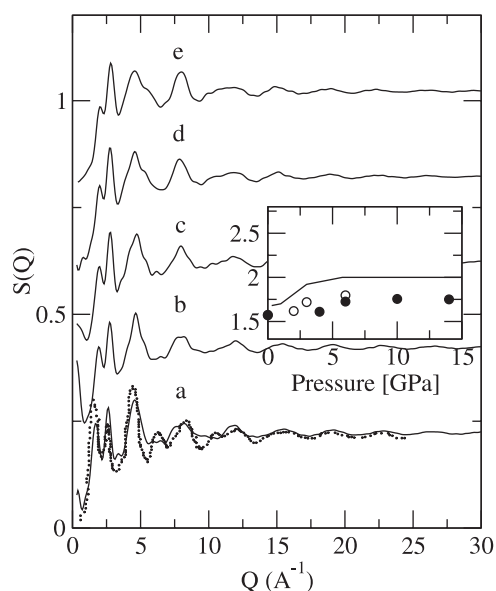


Figure 5. Scattering factor $S(Q)$ for different applied pressures: (a) 0 GPa, (b) 3.0 GPa, (c) 5.76 GPa, (d) 8.92 GPa and (e) 16.6 GPa. The lower curve (a) is the virgin system at 0 GPa, compared to experiments [9]. The inset shows the simulated position in Q_P of the FSDP with pressure (full curve). Experimental data are from [28] (open circles) and [9] (full circles).

the tetrahedra sets in, which in turn stabilizes more or less the Ge–O–Ge bond angle. The sharp increase of the δ_{Ge} at 3 GPa deserves some comments as one may argue that it is a signature of a first-order amorphous–amorphous transformation [20]. First, one should note that the position of the moderate jump at ≈ 5 GPa in the present simulated silica can be well correlated with the vanishing of low frequency modes [18]. This leads to the identification of a floppy to rigid transition [17] that is here induced by the increasing silicon coordination number. On the other hand, the usual phenomenology of floppy to rigid transitions having the mean coordination number as the order parameter [26] can be entirely translated in terms of pressure, as recently shown for reversibility windows [24]. Since germanium dioxide is a structural analogue of silica, this transition [27] occurs in the same way but at lower P because of the increased sensitivity of GeO_2 under pressure change.

Further interpretation is provided from the variation of the position of the FSDP with respect to pressure. In figure 5 are represented the scattering functions for different applied pressures which show a global broadening of the peak at 4 \AA^{-1} whereas the position of the FSDP at 1.5 \AA^{-1} is shifted to higher values in Q , already at very low pressure and even before the angular drop at $P = 1.8$ GPa. With increasing pressure, the calculated FSDP broadens and becomes less intense, as currently observed from x-ray or neutron diffraction [11]. It is worth noting that the peak at 2.5 \AA^{-1} obtained in the present simulation is only weakly observable in the experiments from neutron diffraction [9] displayed in figure 5. However, the simulated double peak distribution between 1.5 and 2.5 \AA^{-1} has been observed by different authors [29] (see also the discussion in [12]). The evolution with pressure of the position Q_P of the FSDP is represented in the inset of figure 4. Both experiments and simulation show that Q_P already increases at low pressures and then stabilizes at around $Q = 1.7 \text{ \AA}^{-1}$ ($\approx 2 \text{ \AA}^{-1}$ in the simulation). This suggests that intermediate-range order is immediately affected by the densification and then remains unaffected with further densification.

In conclusion, we have shown that simulated GeO₂ under pressure shows several main features with applied pressure and pressure release:

- (i) a global increase of the number of oxygen neighbours in the vicinity of a germanium atom,
- (ii) a stepwise change in the local structure with applied pressure, made up of a reduction of long-range correlation (seen from the position of the FSDP), a sharp reduction of the intertetrahedral bond angle and then a progressive distortion of the GeO_{4/2} tetrahedron, and
- (iii) no noticeable change in bond distance between a virgin and a permanently densified system but significant differences in bond angles.

This clearly draws the following picture: pressure applies on different length scales. With increasing magnitude, densification is realized by a successive deformation of long-range structure, intermediate-range structure (angular) and finally short-range structure (tetrahedral).

It is a pleasure to acknowledge instructive discussions with Yves Guissani and Bertrand Guillot. The author also thanks K Trachenko for sharing some results on reversibility windows in GeO₂. The Laboratoire de Physique Théorique des Liquides is Unité Mixte de Recherche no 7600 du CNRS.

References

- [1] Gill R 1996 *Chemical Fundamentals of Geology* (New York: Kluwer–Academic)
- [2] Spera F J 1989 *Geology* **17** 388
- [3] Brueckner R 1970 *J. Non-Cryst. Solids* **5** 123
- [4] Hemley R J, Mao H K, Bell P M and Mysen B O 1986 *Phys. Rev. Lett.* **57** 747
- [5] Williams Q and Jeanloz R 1988 *Science* **239** 902
- [6] Guissani Y and Guillot B 1996 *J. Chem. Phys.* **104** 7633
- Horbach J, Kob W and Binder K 2001 *Chem. Geol.* **174** 87
- [7] Laubengayer A W and Morton D S 1932 *J. Am. Ceram. Soc.* **54** 2303
- [8] Itié J P, Polian A, Calas G, Petiau J, Fontaine A and Tolentino H 1989 *Phys. Rev. Lett.* **63** 398
- [9] Stone C, Hannon A C, Ishihara T, Kitamura N, Shirakawa Y, Sinclair R N, Umesaki N and Wright A C 2001 *J. Non-Cryst. Solids* **293–295** 769
- [10] Murthy M K and Ip J 1964 *Nature* **201** 285
- [11] Price D L, Saboungi M L and Barnes A C 1998 *Phys. Rev. Lett.* **81** 3207
- [12] Price D L, Ellison A J G, Saboungi M L, Hu R Z, Egami T and Howells W S 1997 *Phys. Rev. B* **55** 11249
- [13] Henderson G S and Fleet M E 1991 *J. Non-Cryst. Solids* **134** 259
- [14] Oeffner R D and Elliott S R 1998 *Phys. Rev. B* **58** 14791
- [15] Tsuchiya T, Yamanaka T and Matsui M 1998 *Phys. Chem. Minerals* **25** 94
- [16] Meade C, Hemley R J and Mao H K 1992 *Phys. Rev. Lett.* **69** 1387
- [17] He H and Thorpe M F 1985 *Phys. Rev. Lett.* **54** 2107
- [18] Trachenko K and Dove M 2002 *J. Phys.: Condens. Matter* **13** 1143
- [19] Vashishta P, Kalia R and Ebbsjö I 1989 *Phys. Rev. B* **39** 6034
- [20] Lacks D J 2000 *Phys. Rev. Lett.* **84** 4629
- [21] Sampath S, Benmore C J, Lantzky K M, Neufeind J, Leinenweber K, Price D L and Yarger J L 2003 *Phys. Rev. Lett.* **90** 115502
- [22] Price D L, Ross S C, Reijers R, Susman M L and Saboungi M L 1989 *J. Phys.: Condens. Matter* **1** 1005
- [23] Trachenko K, Dove M T, Hammonds K D, Harris M J and Heine V 1998 *Phys. Rev. Lett.* **81** 3431
- [24] Trachenko K and Dove M T 2003 *Phys. Rev. B* **67** 064107
- [25] Tsuneyucki S, Tsukada M, Aoki H and Matsui Y 1988 *Phys. Rev. Lett.* **61** 869
- [26] Boolchand P, Feng X and Bresser W 2001 *J. Non-Cryst. Solids* **293** 348
- [27] Trachenko K 2004 private communication
- [28] Sugai S and Onodera A 1996 *Phys. Rev. Lett.* **77** 4210
- [29] Waseda Y, Sugiyama K, Matsubara E and Harada K 1990 *Mater. Trans. JIM* **31** 421